An Energy Compensation Approach to Variable Stiffness Single Leg Jumping

1st Mohammadreza Gilak
Department of Electrical Engineering
Sharif University of Technology
Tehran, Iran
mohammadreza.gilak@ee.sharif.edu

2nd Mehdi Zarei
Department of Mechanical Engineering
Sharif University of Technology
Tehran, Iran
mehdi.zar@student.sharif.edu

3rd Saman Samiei
Department of Aerospace Engineering
Sharif University of Technology
Tehran, Iran
saman.samiei@ae.sharif.edu

4th Mohammad Hossein Basiri
Department of Electrical Engineering
Amirkabir University of Technology
Tehran, Iran
basiri@aut.ac.ir

5th Mohammad Mehdi Jalalmaab
Fasta Robotics Inc.
Sharif Science and Technology Park
Tehran, Iran
mjalalmaab@fasta.technology

6th Behzad Ahi
Department of Electrical Engineering
Sharif University of Technology
Tehran, Iran
ahi@sharif.edu

7th Hassan Haddadpour
Department of Aerospace Engineering
Sharif University of Technology
Tehran, Iran
haddadpour@sharif.edu

***Abstract*—In this study, we propose a phase-based control framework consisting of a flight-phase Bézier-curve foot trajectory controller and a stance-phase variable-stiffness spring model for stable and dynamic locomotion of a quadruped robot's single leg under frictional contact conditions. The approach employs a bio-inspired spring-loaded inverted pendulum template to capture the fundamental characteristics of animal-like jumping gaits. During the flight phase, smooth transitions are achieved through the generation of foot-end trajectories and leg orientation control, both parameterized using Bézier curves. In the stance phase, a variable-stiffness spring model is incorporated to compensate for energy dissipation caused by friction. Comprehensive simulation results validate the effectiveness of the proposed controller in preserving jumping performance by mitigating energy losses. Furthermore, the findings indicate that iterative adaptation of spring stiffness significantly reduces the adverse effects of friction.**

***Index Terms*—Spring-loaded inverted pendulum, single-leg locomotion, quadrupedal robots, Bézier curves, hopping platform**

I. Introduction

Given the rapid growth of robotics technology and the expansion of its applications in diverse fields such as medicine, transportation, agriculture, and manufacturing industries, the need for intelligent, robust, and reliable robotic systems is increasingly felt [1]. Among the various types of robots, legged robots have gained a special position in research and practical applications due to their ability to move in uneven environments and to simulate the locomotion behavior of humans and animals [2], [3]. Recent studies have even demonstrated their utility in challenging environments such as ocean exploration [4]. The optimal performance of legged robots is directly tied to the quality of their control algorithms. The design and development of efficient control strategies not only enhance locomotion accuracy and speed but also improve the system's reliability, stability, and adaptability. However, due to the nonlinear nature of their dynamics, the presence of uncertainties, and complex interactions with the environment, controlling legged robots remains one of the fundamental challenges in robotics [5], [6].

A fundamental advantage of legged robots over wheeled robots is their ability to traverse uneven terrain. This benefit is rooted in the decoupling between the robot's body and the environment. First, the movement of the robot's body becomes largely independent of the terrain's smoothness or roughness, as in many cases, the legs act as an active suspension system between the body and the ground. Second, this decoupling allows the legs to temporarily detach from the ground, enabling access to locations that would otherwise be completely unreachable under different conditions. But these advantages come at the cost of more complicated dynamics and dealing with hybrid systems in control design.

In recent years, several studies have sought to improve the control of legged robots. For instance, Tian et al. [7] employed fast quadratic programming processing to control a single joint. Some approaches also attempt to regulate the force exerted by the robot on the ground, aiming for more refined motion that contributes to the robot's longevity. This can be done by either measuring the foot force or estimating the force acting on the robot using a filter, which can then be incorporated into the controller design process [8]. However, these methods rely heavily on a precise model of the leg, which

usually cannot be ensured in real-world applications. While such force regulation approaches are effective for managing contact forces, bio-inspired locomotion models provide an alternative perspective by capturing the compliant dynamics of legged locomotion.

To have the robotic leg interact with the environment, one approach is to incorporate compliant behavior in the actual leg. Lou et al. [9] proposed an energy-based rest length regulation for control of a compliant one-legged robot. Some robots can even switch between two modes of configurations, one of which is compliant [10]. Although physical compliance in robotic legs can improve ground contact behavior, incorporating passive elastic elements may introduce practical challenges such as increased mechanical complexity and limited stiffness adaptability, which can restrict motion flexibility in some robotic designs. Another method of dealing with the problem of contacting the ground in legged robots is incorporating a bio-inspired model called Spring-Loaded Inverted Pendulum (SLIP) model. Huang et al. [11] combined the SLIP model with air trajectory planning for controlling a single leg with three degrees of freedom. The concept of SLIP can also be extended to three-dimensional models [12], wheeled single legs [13], and even quadrupedal robots [14]. Single-leg models are commonly used to study the fundamental dynamics of legged locomotion, as they capture the essential energy exchange and ground interaction behavior while avoiding the additional complexity of multi-leg coordination. Therefore, focusing on a single-leg system provides a suitable framework for investigating friction-induced energy dissipation and evaluating the proposed control strategy before extending it to full quadruped systems.

Building upon this foundation, we present a control algorithm that integrates SLIP-based modeling with air trajectory planning, complemented by a novel method for computing thrust force during the stance phase. This approach allows the controller to effectively compensate for energy dissipation caused by friction in the flight phase, thereby enhancing the overall stability and efficiency of legged locomotion.

The rest of the paper is organized as follows. Sec. II reviews basic concepts such as impedance control and Bézier curves. Sec. III presents the kinematics and dynamics of the single-leg robot together with the SLIP model. Sec. IV describes the control design. Simulations are presented in Sec. V. Finally, Sec. VI concludes the paper.

II. Preliminaries

A. Impedance Control

Legged robots must constantly control how they interact with the ground. Unlike wheeled robots, each leg repeatedly enters and leaves contact with environments that can be stiff, soft, compliant, uneven, or even moving. Leg control cannot rely purely on precise trajectory tracking, since the forces exerted by the ground on the robot are only partly predictable. Instead, the leg must balance the two objectives of allowing some deviation from planned motion so that unexpected contact forces do not destabilize the robot, and generating appropriate forces to support body weight, to attain locomotion, and to reject disturbances.

Impedance control provides a natural and physically intuitive framework for meeting these requirements. Impedance control, in the context of a single robotic leg, controls the dynamic relation between the motion of the leg and the ground reaction forces arising from stance and impact. Rather than commanding forces directly or attempting to track position rigidly, the controller shapes how the leg behaves mechanically, much like a tunable mass-spring-damper system. This desired impedance behavior in a robot can be achieved in different ways. One solution is to employ springs and dampers in the structure of the robot [9]. Another option is to make the robot behave as an impedance using the control inputs. Any mechanical behavior can be imitated using only the control inputs.

Here, impedance is realized at the joint level of the robot. This design choice stems from the use of motors equipped with intrinsic field-oriented control, which obviates the need for low-level current regulation. Therefore, instead of using a rigid controller for reference tracking, a proportional-derivative controller is used as

$$\tau = \tau_{ff} + K_p(q_{des} - q) + K_d(\dot{q}_{des} - \dot{q}), \tag{1}$$

where τ_{ff} is the feed-forward torque used to compensate for gravity and to account for the stance-phase dynamics, while during the swing phase the desired joint position and velocity are tracked through the PD terms. K_p and K_d are the position and velocity gains, q_{des} and $\dot{q}_{des}$ are the desired joint angle and angular velocity, and q and $\dot{q}$ are the joint angle and angular velocity, respectively. In the proposed framework, the desired impedance behavior is approximated through the SLIP representation, where the compliant leg is modeled as a spring whose stiffness governs the interaction dynamics during stance.

B. Bézier Curves

Bézier curves are an important class of functions used in computers, graphics, motion planning, and even vehicle design. They have the feature that their derivatives of any order can also be specified at any point along the curve by using special points called control points. A Bézier curve of order n has $n+1$ control points.

The first-order Bézier curve is just a line between the two control points, given by

$$B_1(t) = (1-t)P_0 + tP_1, \ , 0 \le t \le 1, \tag{2}$$

in which P_0 and P_1 are the control points. The second-order Bézier curve is defined as

$$B_2(t) = (1-t)B_1^{P_0,P_1}(t) + tB_1^{P_1,P_2}(t), \ , 0 \le t \le 1, \tag{3}$$

where this time P_0, P_1 and P_2 are the three control points. Higher-order Bézier curves are defined recursively in a similar manner. The equivalent polynomial representation using Bernstein basis functions is commonly used to express Bézier

curves of arbitrary order. In the context of this paper, 5th-order Bézier curves are used to ensure a smooth foot trajectory during the flight phase.

III. Modelling

A. Kinematics

The single leg investigated in this paper is a planar robot with two degrees of freedom. It consists of a hip joint mounted on a vertical slider and a knee joint. The kinematic structure of the leg is illustrated in Fig. 1, where the hip and knee joint angles are denoted by q_1 and q_2, respectively. The Cartesian position of the foot tip relative to the hip joint is expressed as

$$x(q_1, q_2) = -l_1 \cos(q_1) - l_2 \cos(q_1 + q_2), \tag{4}$$

$$y(q_1, q_2) = -l_1 \sin(q_1) - l_2 \sin(q_1 + q_2). \tag{5}$$

A fundamental tool in robotics is the Jacobian matrix since it relates joint velocities to end-effector velocities. The Jacobian is essential for tasks like control, inverse kinematics, and force mapping. Here, we consider the foot as the end effector, and since its orientation is not of interest, we can write

$$\dot{x}(q_1, \dot{q}_1, q_2, \dot{q}_2) = l_1 \dot{q}_1 \sin(q_1) + l_2(\dot{q}_1 + \dot{q}_2) \sin(q_1 + q_2), \tag{6}$$

$$\dot{y}(q_1, \dot{q}_1, q_2, \dot{q}_2) = -l_1 \dot{q}_1 \cos(q_1) - l_2(\dot{q}_1 + \dot{q}_2) \cos(q_1 + q_2). \tag{7}$$

The Jacobian is the matrix of partial derivatives of the end-effector position with respect to the joint angles.

$$J = \begin{bmatrix} l_1 \sin(q_1) + l_2 \sin(q_1 + q_2) & l_2 \sin(q_1 + q_2) \\ -l_1 \cos(q_1) - l_2 \cos(q_1 + q_2) & -l_2 \cos(q_1 + q_2) \end{bmatrix} \tag{8}$$

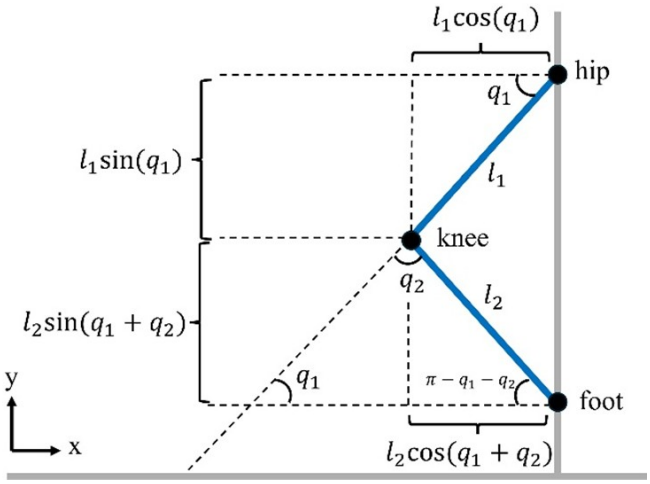

Fig. 1. Planar kinematics of the two-DOF robotic leg.

B. Dynamics

The dynamics of the robotic leg are modeled as a two-link serial mechanism in the hip-attached frame. The equations of motion are expressed in the standard manipulator form

$$M(q)\ddot{q} + C(q, \dot{q})\dot{q} + G(q) = \tau + J^T(q)F, \tag{9}$$

where $q = [q_1, q_2]^T$ is the vector of joint angles, $M(q)$ is the inertia matrix, $C(q, \dot{q})\dot{q}$ contains the Coriolis and centrifugal terms, and $G(q)$ is the gravity vector. The vector τ denotes the applied actuator torques.

In this formulation, F represents the ground reaction force acting at the foot, and the Jacobian matrix $J(q)$ is defined in (8). During the stance phase, the force computed by the SLIP template model (described in Sec. IV) is substituted for F. During the swing phase, when the foot is not in contact with the ground, the contact force is zero.

C. Spring-Loaded Inverted Pendulum Modelling

In the field of legged robotics, it is common practice to draw inspiration from biological systems. One widely adopted bio-inspired model is the SLIP, which captures the essential dynamics of running gaits observed in many quadrupedal animals. In this framework, the leg is abstracted as a massless spring connected to a point mass representing the body. This simplified representation reproduces the characteristic behaviors of animal locomotion. Importantly, the SLIP model exhibits hybrid dynamics: during the flight phase, the mass evolves under the influence of gravity, while ground contact initiates the compression phase. In this phase, the vertical velocity of the center of mass is negative, the spring compresses, and mechanical energy is stored as elastic potential energy. As the spring subsequently extends, the system transitions into the thrust phase, releasing the stored energy as kinetic energy and propelling the mass upward. In the absence of external perturbations, the compression and thrust phases are dynamically symmetric.

For animals, horizontal running speed can be modulated by adjusting the touchdown angle, defined as the hip angle at the instant of ground contact. Due to the mechanical constraints of the experimental test stand, the system is restricted to vertical motion and horizontal translation is not allowed. Therefore, the horizontal velocity is fixed at zero and the touchdown angle is kept constant at 0°. Consequently, the study focuses on vertical hopping dynamics and energy compensation rather than speed modulation through touchdown angle adjustment. The maximum vertical displacement, or apex height, achieved during locomotion depends on the stiffness and nominal length of the spring, which govern the energy storage and release characteristics of the system. In the SLIP representation, the robot body is modeled as a point mass located at the hip. The virtual leg length l corresponds to the distance between the hip and the foot, which is determined by the joint configuration (q_1, q_2) through the kinematic relations.

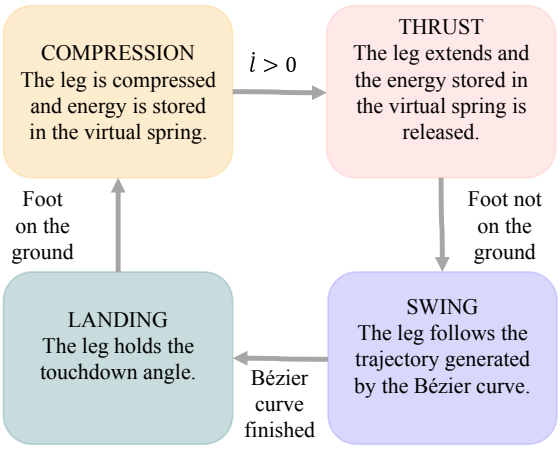

Fig. 2. Finite state machine of the controller.

IV. Controller Design

The controller employed here bears close resemblance to that of Huang et al. [11], whose approach has become widespread within the legged robotics literature. A four-state finite state machine governs the motion. The first state, compression, corresponds to the phase in which the leg behaves like a spring being compressed and accumulating elastic energy. The second state, thrust, follows as the leg begins to extend, driven by the force stored during compression. The third state, swing, is characterized by the foot-end tracking a trajectory generated via Bézier curves. The final state, landing, occurs once the Bézier curve timing has elapsed and the virtual spring has returned to its nominal length, preparing the leg for touchdown. The finite state machine is shown in Fig. 2. During the swing phase, the foot follows a 5th-order Bézier curve, whose six control points are defined as

$$P = \begin{bmatrix} x_{lo} & x_{lo} & x_{lo} & x_{lo} & x_{td} & x_{td} \\ y_{lo} & y_{lo} & y_{lo}+H & y_{lo}+H & y_{td} & y_{td} \end{bmatrix}, \quad (10)$$

where (x_{lo}, y_{lo}) and (x_{td}, y_{td}) respectively are the lift-off and the touchdown coordinates, and H is a tunable variable, allowing the robot to increase the clearance of the leg, in cases of needing higher jumps or avoiding obstacles. The Bézier curve generated with the control points in (10) defines a desired trajectory for the foot-end. The repetition of some control points is intentional and is used to shape the boundary behavior of the trajectory, ensuring smooth take-off and landing transitions during the swing phase. This trajectory is transformed into joint angles and angular velocities using the inverse kinematics of the leg. The controller in (1) is then used to follow this trajectory.

The generated Bézier curve also includes time, meaning it is a trajectory, not a path. This means it might end before the foot has reached the ground. This is where the landing phase comes in. In the landing phase, the leg holds its configuration, so that the spring is at nominal length and the touchdown angle is preserved. The landing phase also utilizes (1) to keep the desired pose.

When the foot makes contact with the ground, it enters the compression phase. In this phase, the controller regulates the leg–ground interaction force based on the dynamic model, where the desired force replaces the ground reaction force appearing in the dynamic model. A virtual spring system is considered and the force produced by this structure is calculated as

$$F_{sd} = K_s(l - l_{des}), \quad (11)$$

where l is the length of the virtual spring considered at the foot, l_{des} is the length of the virtual spring at rest and K_s is the spring coefficient. This force acts to decelerate the downward motion of the leg, thereby softening the impact at touchdown.

As the spring begins to extend back toward its nominal length, the system transitions into the thrust phase. The same force model applies, but with a modified stiffness coefficient, defined as

$$K_s' = K_s + \Delta K, \quad (12)$$

in which ΔK is calculated such that enough energy is added to the system so that the system can reach its desired apex height. Assuming the apex condition where the vertical velocity of the center of mass becomes zero, the injected elastic energy is converted into gravitational potential energy. Therefore, the additional energy introduced by the virtual spring can be expressed as

$$\frac{1}{2}\Delta K(l_{\min} - l_{des})^2 = mg\Delta h, \quad (13)$$

where $\Delta h = h_{des} - h$ represents the height error relative to the desired apex. At maximum compression, when $l = l_{\min}$, the system stores all of its energy in the spring, with no gravitational potential energy present. Furthermore, the effects of slider and joint frictions can then be mitigated by updating the spring constant at every sample, because every time the leg doesn't reach the desired height due to friction, the spring constant changes to compensate for that. From (13), ΔK can be computed as

$$\Delta K = \frac{2mg\Delta h}{(l_{\min} - l_{des})^2}. \quad (14)$$

While a complete Poincaré map analysis is out of the scope of this paper, extensive simulations have been done to show the effectiveness of the method.

V. Simulation Analyses

In this section, the proposed control scheme is examined in detail. All simulations are carried out in the Isaac simulation environment, chosen for its high-fidelity physics engine and precise numerical accuracy. The behavior of the robotic leg across different locomotion phases is illustrated in Fig. 3, which provides a visual representation of the leg's configuration during swing, landing, compression, and thrust. Two sets of simulations were carried out. In the first experiment, friction was taken into consideration to model the real-world system accurately; however, no compensation strategy was

Fig. 3. Simulation of the robotic leg in the Isaac environment, illustrating the leg model during different phases of locomotion.

applied. In the second experiment, the proposed approach was implemented to counteract the energy dissipation due to friction. This was achieved by injecting additional energy during the thrust phase, thereby restoring the system's ability to reach the desired apex height.

The experimental results are shown in Fig. 4, for which hip height is used as a measure of jumping ability, because it is well established in this context as an appropriate indicator of robotic agility and performance. In the frictionless case, the leg attains its maximum jump height. If friction is present, the leg cannot support the same height of jumping; its energy is progressively dissipated over a few cycles, and the motion eventually ceases completely. In contrast, when the proposed method is applied, despite continuous energy losses due to friction, the robot is able to sustain repeated jumping by means of energy injection during the thrust phase, whereas without compensation the motion gradually decays due to dissipative effects. It can be seen that the desired jumping height is achieved in a few cycles. The variation of the spring constant is illustrated in Fig. 5. Initially, the stiffness undergoes a sharp adjustment to enable the leg to reach the desired apex height. Subsequently, it converges to a steady value that compensates for energy losses in the system, ensuring consistent performance across successive cycles.

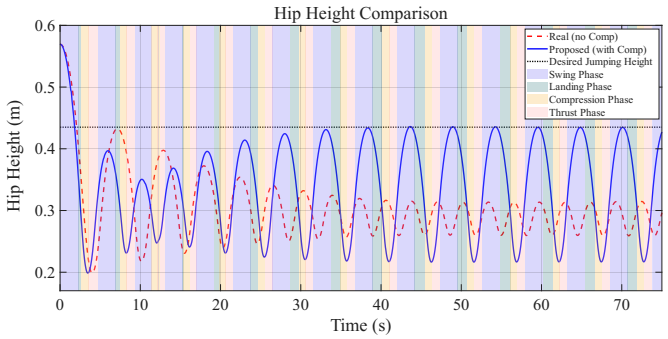

Fig. 4. Comparison of hip apex height across the two simulation experiments. The plot highlights the difference between the uncompensated case, where friction reduces the achieved height, and the compensated case, where additional energy injected during the thrust phase restores the desired apex.

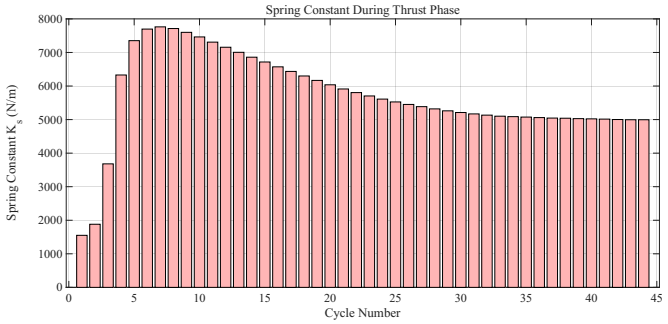

Fig. 5. Variation of the spring constant across successive thrust phases. The plot illustrates how the stiffness is adaptively updated in different cycles to compensate for energy losses and ensure the desired apex height is achieved.

VI. Conclusion

This paper introduced a novel energy-conservation-based approach for achieving a desired apex height in a single-leg robotic platform. The proposed method employs a finite state machine controller in which the spring stiffness is adaptively varied during the thrust phase. Extensive simulation studies validated the effectiveness of the approach, demonstrating its ability to compensate for energy losses and maintain consistent performance. Future research will focus on establishing a more rigorous analytical proof of stability and extending the framework to incorporate additional terms to mitigate the frictional effects.

References

[1] I. Al-Tameemi and O. Amanuel, "Bipedal robots: A systematic review of dynamical models, balance control strategies, and locomotion methods," *Journal of Robotics and Control*, vol. 6, no. 3, pp. 1240–1254, 2025.

[2] J. Reher and A. D. Ames, "Dynamic walking: Toward agile and efficient bipedal robots," *Annual Review of Control, Robotics, and Autonomous Systems*, vol. 4, no. 1, pp. 535–572, 2021.

[3] Y. Tong, H. Liu, and Z. Zhang, "Advancements in humanoid robots: A comprehensive review and future prospects," *IEEE/CAA Journal of Automatica Sinica*, vol. 11, no. 2, pp. 301–328, 2024.

[4] H. Yang, Y. Din, Q. Liu, and H. Zhang, "Control of a single-leg robot based on closed-loop PD-type iterative learning and neural network," *2024 International Conference on Advanced Control Systems and Automation Technologies (ACSAT)*, pp. 170–177, 2024.

[5] F. N. Martins, "Smart robotics for automation," *Sensors*, vol. 24, no. 12, p. 3900, 2024.

[6] M. Sombolestan and Q. Nguyen, "Adaptive-force-based control of dynamic legged locomotion over uneven terrain," *IEEE Transactions on Robotics*, vol. 40, pp. 2462–2477, 2024.
[7] D. Tian, J. Gao, C. Liu, and X. Shi, "Simulation of upward jump control for one-legged robot based on QP optimization," *Sensors*, vol. 21, no. 5, p. 1893, 2021.
[8] Y. Fan, Z. Pei, and Z. Tang, "Variable impedance control for a single leg of a quadruped robot based on contact force estimation," *International Journal of Control, Automation and Systems*, vol. 22, no. 4, pp. 1360–1370, 2024.
[9] G. Luo, R. Du, S. Song, H. Yuan, Z. Huang, H. Zhou, and J. Gu, "Stable and fast planar jumping control design for a compliant one-legged robot," *Micromachines*, vol. 13, no. 8, p. 1261, 2022.
[10] F. Nan, H. Kolvenbach, and M. Hutter, "A reconfigurable leg for walking robots," *IEEE Robotics and Automation Letters*, vol. 7, no. 2, pp. 1308–1315, 2021.
[11] S. Huang and X. Zhang, "Controlling a one-legged robot to clear obstacles by combining the slip model with air trajectory planning," *Biomimetics*, vol. 8, no. 1, p. 66, 2023.
[12] B. Han, H. Yi, Z. Xu, X. Yang, and X. Luo, "3d-slip model based dynamic stability strategy for legged robots with impact disturbance rejection," *Scientific Reports*, vol. 12, no. 1, p. 5892, 2022.
[13] J. Gao, H. Jin, L. Gao, Y. Zhu, J. Zhao, and H. Cai, "Jump control based on nonlinear wheel-spring-loaded inverted pendulum model: Validation of a wheeled-bipedal robot with single-degree-of-freedom legs," *Biomimetics*, vol. 10, no. 4, p. 246, 2025.
[14] M. S. U. Hassan, D. Vasquez, H. Asif, and C. Hubicki, "Stable and robust slip model control via energy conservation-based feedback cancellation for quadrupedal applications," *arXiv preprint arXiv:2511.05402*, 2025.